

Experimental and Computational Chemistry studies on the inhibition of the Corrosion of Mild Steel in H₂SO₄ by (2s,5s,6r)-6-(2-(aminomethyl)-5-(3-(2-chlorophenyl)isoxazol-5-yl)benzamido)-3,3-dimethyl-7-oxo-4-thia-1-azabicyclo[3.2.0]heptane-2-carboxylic acid

Nnabuk O. Eddy^{1,*}, Eno E. Ebenso², Udo J. Ibok³, Emem E. Akpan⁴

¹Department of Chemistry, Ahmadu Bello University, Zaria, Nigeria.

²Department of Chemistry, School of Mathematical and Physical Sciences, North-West University (Mafikeng Campus), Private Bag X2046, Mmabatho 2735, South Africa

³Department of Chemistry, University of Calabar, PMB 1115, Calabar, Nigeria

⁴Department of Computer Science, Federal Polytechnic, Nasarawa, Nigeria

*E-mail: nabukeddy@yahoo.com

Received: 20 July 2011 / Accepted: 15 August 2011 / Published: 1 September 2011

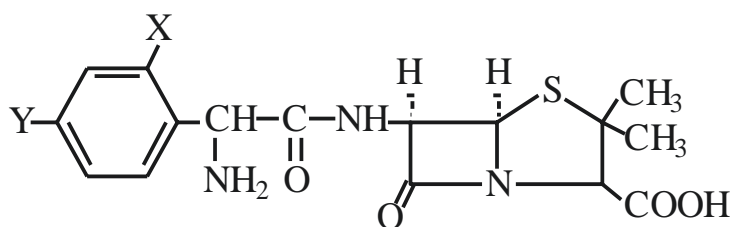
Inhibition of the corrosion of mild steel in 0.1 M H₂SO₄ by (2S,5S,6R)-6-(2-(aminomethyl)-5-(3-(2-chlorophenyl)isoxazol-5-yl)benzamido)-3,3-dimethyl-7-oxo-4-thia-1-azabicyclo[3.2.0]heptane-2-carboxylic acid (AMPX) was studied using experimental (gravimetric, gasometric and thermometric methods) and quantum chemical methods. The results obtained from the experiments revealed that the %inhibition efficiencies at various concentrations of AMPX decrease with increase in temperature but increased with increasing concentrations. The adsorption of the inhibitor on mild steel surface is spontaneous and supported the Langmuir adsorption model. Synergistic studies between the inhibitor and potassium halides (KI, KBr and KCl) indicated that the inhibition potentials of AMPX can be enhanced through synergistic combinations with halides. Quantum chemical consideration indicated that semi empirical parameters calculated for AMPX are comparable to those of other inhibitors. Results obtained from condensed Fukui function and Huckel charge analyses indicated that the site for electrophilic attack in AMPX is in the amide nitrogen (N14). The energy of interaction and proton affinity for all possible adsorption sites in AMPX have been calculated and from the results obtained, AMPX can easily be protonated, its adsorption is downhill exothermic and preferentially favours the amide nitrogen (N14).

Keywords: Corrosion, inhibition, adsorption, Fukui function, energy of interaction, protonation

1. INTRODUCTION

Corrosion inhibitors are needed in the oil, fertilizer, metallurgical and other industries, where contact between metal and aggressive medium is imperative [1-2]. In order to tackle the menace attributed to corrosion, several measures (including anodic and cathodic protection, lubrication, painting and electroplating) have been adopted. However, one of the best options accessible for the protection of metals against corrosion involves the use of organic inhibitor [3]. Most successful inhibitors are synthesized from cheap raw materials or are selected from compounds, which have hetero atom (N, O, P, S) in their aromatic or long carbon chain [4]. The presence of these hetero atom in the organic compound as well as suitable functional groups and π -electrons facilitate the adsorption of the inhibitor on the metal surface [5].

In our research group, we have studied the inhibition potentials of several plant materials, drugs, amino acids and some hetero cyclic compounds [6-10]. We noted that most aromatic derivatives of carboxylic acid exhibit excellent inhibition potentials for the corrosion of some metals, even at higher concentration of acid and temperature. These classes of compounds are also found to be receptive to quantum chemical modelling. In continuation of our research on the search for better, relatively less toxic and cheaper corrosion inhibitors, the inhibition potentials of (2S,5S,6R)-6-(2-(aminomethyl)-5-(3-(2-chlorophenyl)isoxazol-5-yl)benzamido)-3,3-dimethyl-7-oxo-4-thia-1-azabicyclo[3.2.0]heptane-2-carboxylic acid (AMPX) for mild steel is considered for investigation in this study. Gravimetric, gasometric and thermometric methods are used in the experimental aspect of the study while results obtained from semi empirical, Fukui, Huckel charge and other quantum chemical indices were used to study the mechanism of inhibition, possibility of protonation and interaction. The figure below shows the structure of the inhibitor (AMPX) where X and Y = H. From the structure, it can be seen that AMPX has several hetero atoms including nitrogen, sulphur and oxygen at different positions. Therefore, ampx is expected to be a good corrosion inhibitor.



2. MATERIALS AND METHODS

2.1 Materials

Mild steel sheet of composition (wt %); Mn (0.6), P (0.36), C (0.15) and Si (0.03) and the rest Fe was used for the study. Different coupons of dimension 5 x 4 cm were produced from the primary sheet. Concentration of AMPX used for experimental study ranged from 2×10^{-7} to 10×10^{-7} M. H_2SO_4 concentration of 2.5 M was used for gasometric and thermometric studies while concentration of 0.1 M

was used for gravimetric study. All reagents used for the study were Analar grade and double distilled water was used for their preparation

2.2 Thermometric method

In order to determine the corrosion rate in the different reagents, a three-neck flask with provisions for the introduction of chemicals and for insertion of electronic thermometer was used for thermometric study. For each study, the mild steel coupon was introduced into the flask. Enough quantities of each solution were in turn transferred into the flask until the mild steel coupon was completely immersed. Once this was done, the temperature of the reacting solution was read at one-minute interval until a constant temperature was obtained.

The reaction number (RN) of each system was calculated by dividing the difference between the highest and lowest temperature attained by the time interval while the inhibition efficiency was calculated using equation 1 [11].

$$\% I = \frac{RN_{aq}}{RN_{wi}} \times 100 \quad \mathbf{1}$$

where RN_{aq} is the reaction number in the absence of inhibitors (blank solution) and RN_{wi} is the reaction number of 2.5 M HCl containing the studied inhibitor.

2.3 Gravimetric (Weight loss) method

A previously weighed metal (mild steel) was completely immersed in 250 ml of the test solution in an open beaker. The beaker was inserted into a water bath maintained at a temperature of 30°C. Similar experiments were repeated at 40, 50 and 60°C. In each case, the average weight (from triplicate measurements) of the sample before immersion was measured using Scaltec high precision balance (Model SPB31). After every 24 hours, each sample was removed from the test solution, washed in a solution of NaOH containing zinc dust and dried in acetone before re-weighing. The difference in weight for a period of 168 hours was taken as total weight loss. The inhibition efficiency (%I) for each inhibitor was calculated using the following formula [12];

$$\% I = (1 - W_1/W_2) \times 100 \quad \mathbf{2}$$

where W_1 and W_2 are the weight losses (g/dm^3) for mild steel in the presence and absence of inhibitor in H_2SO_4 solution respectively. Also, the degree of surface coverage θ is given by equation 3 [13];

$$\theta = 1 - W_1/W_2 \quad \mathbf{3}$$

2.4 Gasometric method

In the gasometric method, the test solution was poured into the reaction vessel. Upon the introduction of mild steel, the flask was quickly corked and the rise in volume of the paraffin due to hydrogen gas evolution was noted after every minute until a steady reading was observed. From the volume of hydrogen gas evolved, the inhibition efficiency was calculated using the following equation;

$$\%I = \left(1 - \frac{V_{Ht}^1}{V_{Ht}^o}\right) \times 100 \quad 4$$

where V_{Ht}^1 and V_{Ht}^o are the volumes of H_2 gas evolved at time, 't' for inhibited and uninhibited solutions respectively.

2.5 Quantum chemical calculations

The molecular structure of AMPX was optimized (Figure 1) using Hyperchem release 8 computational chemistry software.

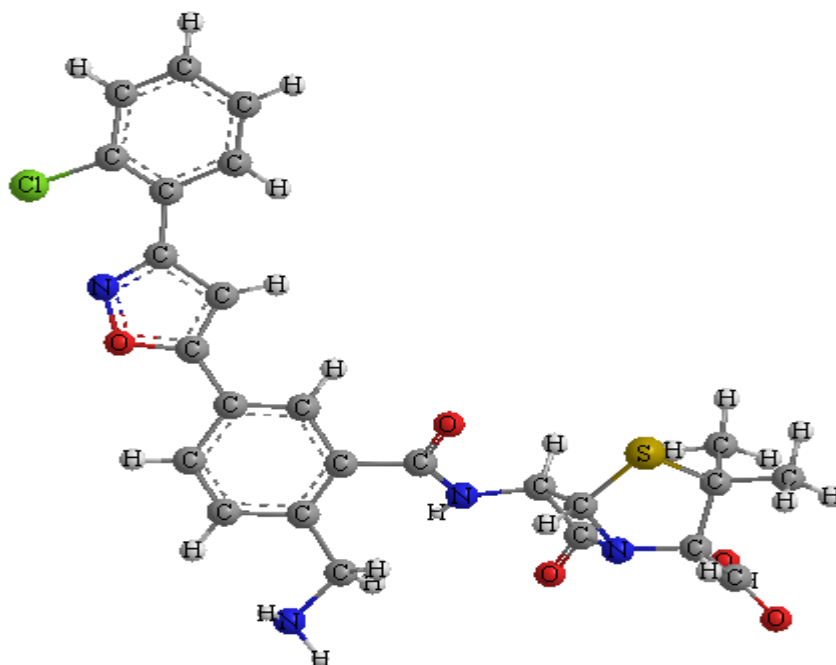


Figure 1. Optimized structure of AMPX

Full geometry optimization was achieved by using molecular mechanics (MM), parametric method 3 (PM3) and density functional theory (DFT/3-2G) in the Hyperchem software. Semi empirical parameters which included the energy of the highest occupied molecular orbital (E_{HOMO}), the energy of the lowest unoccupied molecular orbital (E_{LUMO}), the dipole moment (μ), the total energy

(TE) and the electronic energy of the inhibitor were calculated using MOPAC 2011 computational software. MOPAC calculations were carried out for five different Hamiltonians including parametric model 6 (PM6), parametric model 3 (PM3), Austin model 1 (AM1), Recief model 1 (RM1) and modified neglect of diatomic overlap model (MNDO). Mulliken and Lowdin charges of atoms in the inhibitor were calculated using GAMESS computational soft wares. The correlation type and basic set chosen for the computation were MP2 and Mini respectively.

3. RESULTS AND DISCUSSION

3.1 Effect of concentration of AMPX

Fig. 2 shows the variation of weight loss with time for the corrosion of mild steel in H_2SO_4 containing various concentrations of AMPX at 303 K (plots for 313, 323 and 333 K are not shown).

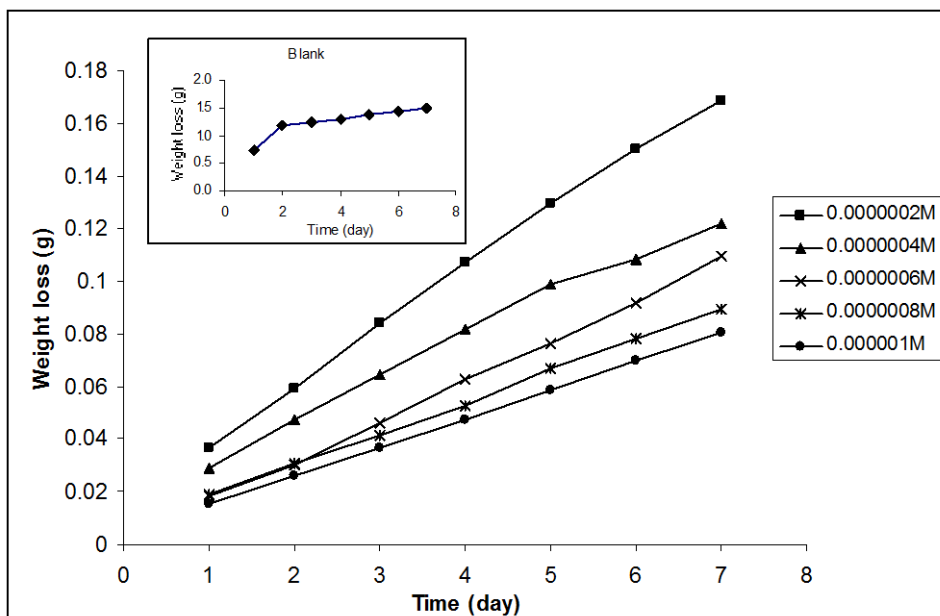


Figure 2. Variation of weight loss with time for the corrosion of mild steel in 0.1 M H_2SO_4 containing various concentrations of AMPX (insert is the plot for the blank)

The Figure indicates that weight loss of mild steel increased with increase in the period of contact and with temperature indicating that the rate of corrosion of mild steel in H_2SO_4 increases with increase in the period of contact and with temperature. However, in the presence of various concentrations of AMPX, weight loss of mild steel was found to decrease with increase in the concentration of AMPX indicating that AMPX retarded the corrosion of mild steel in H_2SO_4 and that AMPX is an adsorption inhibitor for mild steel corrosion [14]. Fig.3 shows the variation of volume of hydrogen gas evolved with time for the corrosion of mild steel in H_2SO_4 containing various concentrations of AMPX at 303 K. From the figure, it is evident that the volume of hydrogen gas

evolved decreases with increase in the concentration of H₂SO₄ confirming that AMPX is an adsorption inhibitor for the corrosion of mild steel in H₂SO₄ [15]. The trends for the variation of temperature with time for the corrosion of mild steel in H₂SO₄ containing various concentrations of AMPX were similar to those obtained from hydrogen gas evolution measurements which also confirmed that AMPX is an adsorption inhibitor for the corrosion of mild steel in H₂SO₄ [16].

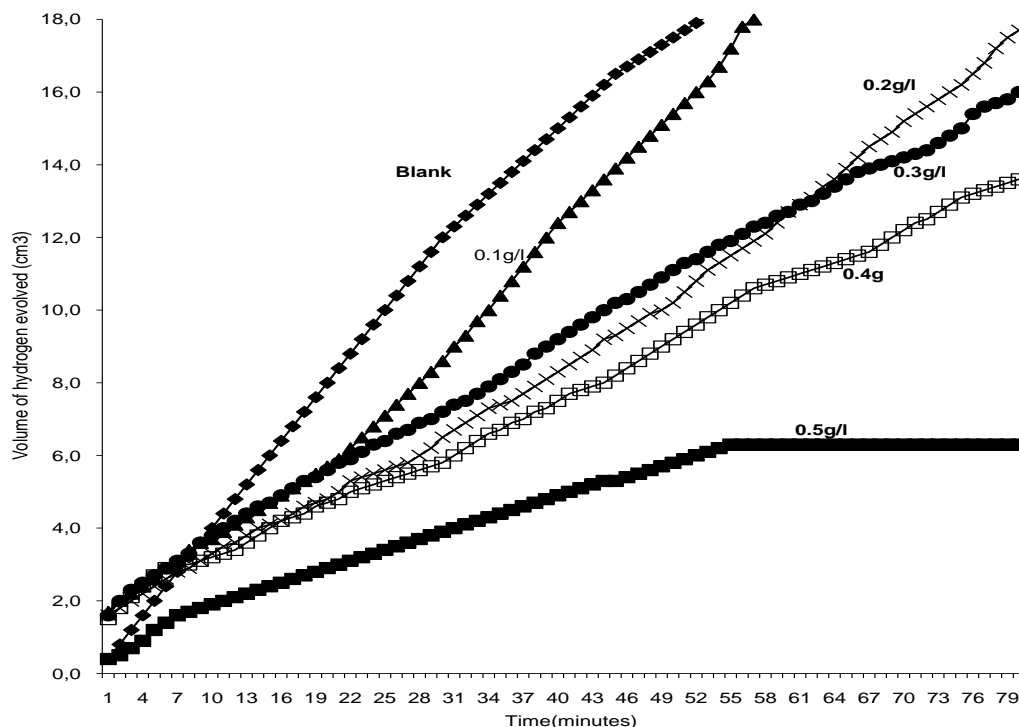


Figure 3. Variation of volume of hydrogen gas evolved with time for the corrosion of mild steel in 0.1M H₂SO₄ containing various concentrations of AMPX

Values of inhibition efficiencies of various concentrations of AMPX (calculated from weight loss, hydrogen evolution and thermometric methods) are presented in Table 1. From the results obtained, it can be seen that while the corrosion rates of mild steel decrease with increasing concentration of AMPX. The inhibition efficiencies increase with increase in the concentration of AMPX indicating that AMPX inhibited the corrosion of mild steel by lowering its corrosion rate. Inhibition efficiency of AMPX was also found to decrease with increase in temperature suggesting that the adsorption of AMPX on mild steel surface follows the mechanism of physical adsorption [16].

The inhibition efficiencies obtained from thermometric and gasometric methods correlated strongly with the data obtained from weight loss ($r = 0.9147$ and 0.9637 for thermometric and gasometric data respectively) indicating strong agreement between the three set of analytical methods. However, data obtained from weight loss measurements were relatively higher than those obtained

from thermometric and gasometric methods. Therefore, the average inhibition efficiency of AMPX is higher than its instantaneous inhibition efficiency [17].

Table 1. Inhibition efficiency of various concentrations of AMPX for the corrosion of mild steel in 0.1 M H₂SO₄

C x 10 ⁻⁷ (M)	Gravimetric				Gasometric	Thermometric
	303 K	313 K	323 K	333 K	303 K	303 K
2	88.76	76.08	76.50	68.65	80.90	74.23
4	91.90	82.43	83.42	75.62	83.30	79.57
6	92.72	82.61	84.25	76.55	86.60	82.18
8	94.05	84.29	88.35	81.76	88.00	88.39
10	94.63	85.57	90.03	83.09	92.80	86.59

3.2 Effect of temperature

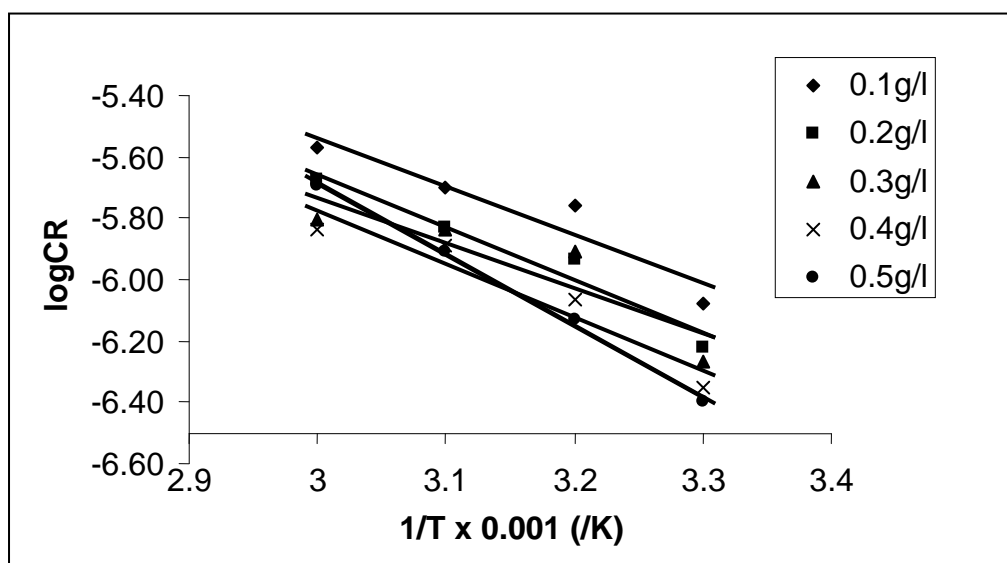


Figure 4. Plots of log CR versus 1/T for the corrosion of mild steel in 0.1 M H₂SO₄ containing various concentrations of AMPX.

The activation energy for the corrosion reaction of mild steel in 0.1 M H₂SO₄ was calculated using the Arrhenius equation [18];

$$CR = A \exp(-E_a/RT) \tag{5}$$

where CR is the corrosion rate of mild steel, A is Arrhenius or pre-exponential constant, E_a is the activation energy for the corrosion reaction of mild steel, R is the gas constant and T is the temperature. Taking the logarithm of both sides of equation 5 yields equation 6:

$$\log(\text{CR}) = \log A - E_a/2.303RT \tag{6}$$

Plots of log(CR) versus 1/T for the corrosion of mild steel in the presence of various concentrations of AMPX yielded straight lines (Fig. 4) indicating that Arrhenius equation is obeyed. From slopes and intercepts of Arrhenius plots, values of E_a and A were computed.

Table 2. Thermodynamic parameters for the adsorption of AMPX on mild steel surface.

C x 10 ⁻⁷ (M)	E _a (J/mol)	R ²	ΔH _{ads} (J/mol)	ΔS _{ads} (J/mol)	R ²
2	30.28	0.8968	27.66	-268.98	0.8794
4	33.04	0.9533	30.42	-263.31	0.9457
6	27.85	0.7853	25.24	-280.02	0.7511
8	32.94	0.9133	30.32	-265.56	0.8999
10	44.57	0.9972	41.95	-228.88	0.9969

Calculated values of E_a (Table 2) ranged from 27.85 to 44.57 J/mol (mean = 33.73 J/mol). The activation energies obtained for the inhibited corrosion reaction of mild steel are lower than 43 kJ/mol suggesting that diffusion process may also controls the rate of adsorption of the inhibitor on mild steel surface and that physical adsorption mechanism is favoured. For a physical adsorption mechanism, the activation energy is expected to be lower than the threshold value of 80 kJ/mol as found in the present results [19].

3.3 Thermodynamic consideration

The transition state equation was used to calculate thermodynamics parameters for the adsorption of AMPX on mild steel surface. This equation shows the relationship between enthalpy of adsorption (ΔH_{ads}), entropy of adsorption (ΔS_{ads}) and corrosion rate (CR) of mild steel as follows [20];

$$\text{CR} = RT(\exp(\Delta S_{\text{ads}}/R)\exp(-\Delta H_{\text{ads}}/RT)/Nh \tag{7}$$

where R is the gas constant, T is the temperature, N is the Avogadro’s number and h is the Planck constant. Rearranging and taking the logarithm of both sides of equation 7 yield equation 8:

$$\log(\text{CR}/T) = \log(R/Nh) + \Delta S_{\text{ads}}/2.303R - \Delta H_{\text{ads}}/2.303RT \tag{8}$$

From equation 8, a plot of log(CR/T) versus 1/T should produce a straight line with slope and intercept equal to ΔH_{ads}/2.303R and (log(R/Nh)+ΔS_{ads}/2.303R) respectively. Values obtained for the corrosion rates of mild steel in the presence of various concentrations of AMPX at 303, 313, 323 and 333K were used for the plot of log(CR/T) versus 1/T and straight lines were obtained (Fig. 5).

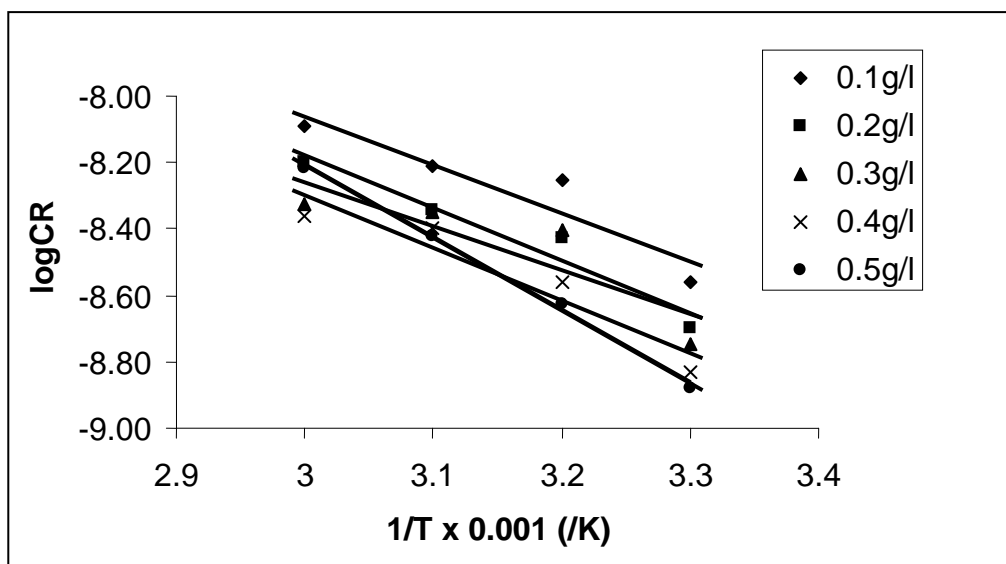


Figure 5. Plots of log (CR/T) versus 1/T for the corrosion of mild steel in 0.1M H₂SO₄ containing various concentrations of AMPX

Values of ΔH_{ads} calculated from slopes of lines on the transition state plots are also recorded in Table 2. These values ranged from 25.24 to 41.95 J/mol indicating that the adsorption of AMPX on mild steel surface is an endothermic process. Also, values of ΔS_{ads} ranged from -228.88 to -280.02 J/mol indicating that the adsorption of AMPX on mild steel surface is characterized by decreasing degree of disorderliness. From thermodynamic point of view, the corrosion of mild steel in the presence of AMPX may be controlled by activation complex and there is association instead of dissociation [21].

3.4 Adsorption isotherm

Adsorption isotherms are very important in determining the mechanism of organo-electrochemical reactions such as corrosion [22]. The most frequently used isotherms are Langmuir, Frumkin, Bockris-Swinkal, El Awarly, Flory Huggins and Temkin adsorption isotherms. The general formula for these isotherms can be expressed as follows;

$$f(0,\alpha)\exp(-2a\theta) = BC \tag{9}$$

where f(0,α) is the configurational factor, θ is the degree of surface coverage, C is the inhibitor concentration in the bulk electrolyte, a is the interaction parameter and B is the equilibrium constant for the adsorption process [23].

Langmuir adsorption isotherm is the ideal adsorption isotherm for physical and chemical adsorption on a smooth surface where there is no interaction between adsorbed molecules and the surface. If it is assumed that the adsorption of AMPX on mild steel surface proceeds according to Langmuir adsorption, then equation 10 is applicable [24];

$$C/\theta = 1/B + C \tag{10}$$

where B is the equilibrium constant of adsorption. The logarithm of both sides of equation 10 yields equation 11:

$$\log(C/\theta) = \log C - \log B \tag{11}$$

From equation 11, a plot of $\log(C/\theta)$ versus $\log C$ should give a straight line with intercept equals to $\log B$ [25].

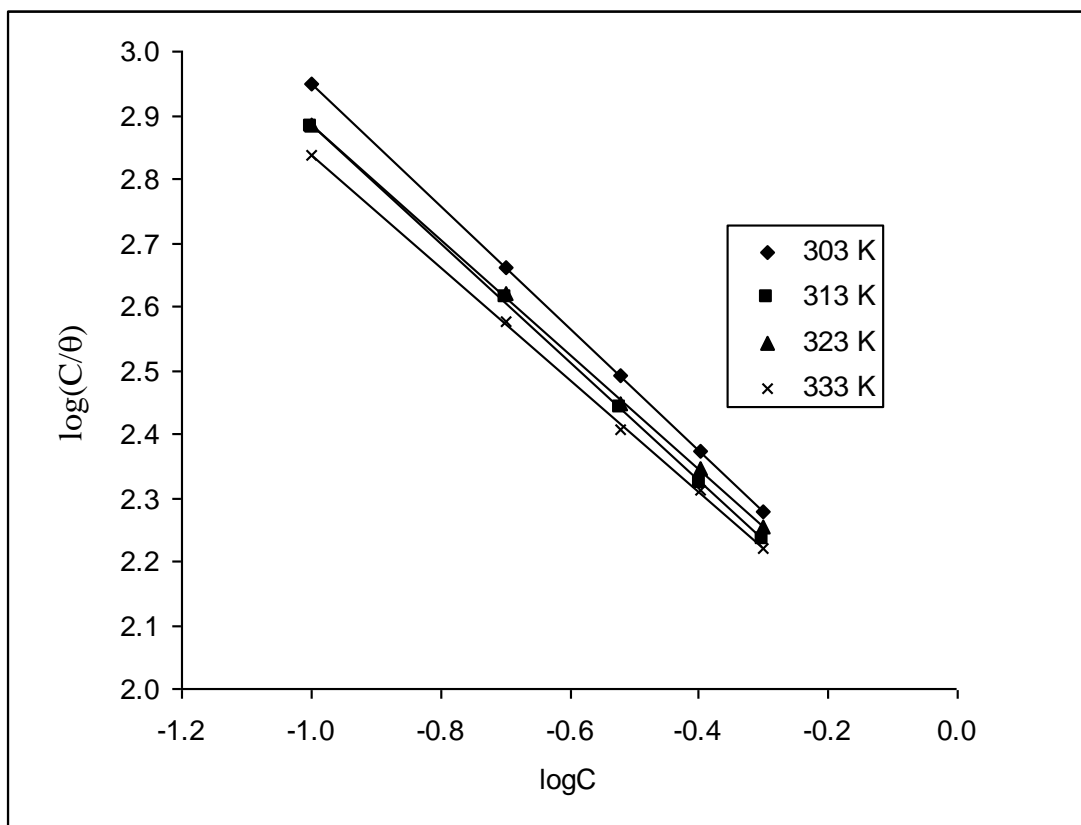


Figure 6. Langmuir isotherm for the adsorption of AMPX on mild steel surface

Fig. 6 shows Langmuir plot for the adsorption of amp on mild steel surface. The application of Langmuir isotherm to adsorption of amp on mild steel surface implies that the addition of AMPX causes a high increase in the free energy for the uninhibited system. These results show strong adsorption of inhibitors on the mild steel surface and suggest the existence of monolayer of adsorption with little or no interaction [26]. The adsorption parameters deduced from Langmuir adsorption isotherm are also presented in Table 3. Values of B were found to decrease with increase in temperature supporting the mechanism of physical adsorption.

Table 3. Langmuir adsorption parameters for the adsorption of AMPX on mild steel surface

Temperature (K)	logK	Slope	ΔG_{ads} (KJ/mol)	R^2
303	0.0111	0.9605	-10.06	1.0000
313	0.0179	0.9043	-10.06	0.9990
323	0.0456	0.9317	-9.86	0.9995
333	0.0588	0.9059	-9.78	0.9935

The free energy of adsorption (ΔG_{ads}) of AMPX on mild steel surface is related to the equilibrium constant of adsorption according to equation 12 [27];

$$\Delta G_{ads} = -2.303RT \log(55.5K) \tag{12}$$

where T is the temperature and K is the equilibrium constant of adsorption. Free energy data calculated from values of B deduced from the Langmuir isotherm are recorded in Table 4. From the results, average values of ΔG_{ads} were negative and are below the threshold value of -40 kJ/mol indicating that the adsorption of AMPX on mild steel surface is spontaneous and occurs by physical adsorption mechanism [28].

Table 4. Inhibition efficiencies of AMPX on addition of halides

$C \times 10^{-7}$ (M)	Gravimetric (303 K)			Gravimetric (333 K)			Thermometric (303 K)			Gasometric (303 K)		
	KBr + AMPX	KI + AMPX	KCl + AMPX	KBr + AMPX	KI + AMPX	KCl + AMPX	AMPX +KI	AMPX +KBr	AMPX +KCl	AMPX +KI	AMPX +KBr	AMPX +KCl
2	94.63	86.88	97.23	86.30	55.41	77.24	77.54	91.23	56.32	87.50	86.54	65.38
4	95.50	90.89	97.69	86.30	70.63	87.63	76.87	93.41	62.34	87.50	86.54	69.22
6	95.23	92.05	98.04	87.87	71.78	87.03	86.63	95.46	38.50	88.46	78.84	74.03
8	96.43	93.52	98.40	91.99	76.56	88.40	50.38	92.92	64.35	89.42	85.57	73.07
10	96.78	95.37	98.55	92.05	78.56	88.45	66.25	92.48	81.49	84.61	87.55	71.15

3.5 Synergistic study

Synergism is a combined action of a compound greater in total effect than the sum of individual effects. It has become one of the most important factors in inhibition process and serves as a basis for all modern corrosion inhibitor formulation. Synergism of corrosion inhibitors is either due to interaction between components of the inhibitors or due to interaction between the inhibitor and one of the ions present in aqueous solution [29]

Synergistic studies have been carried out on combination of 0.06 M KCl, 0.06 M KBr or 0.06 M KI and AMPX. Synergism parameter (S) for joint effect of AMPX and halides has been calculated using equation 13 [30]:

$$S = \frac{1 - I_A - I_B + I_A I_B}{1 - I_{AB}} \tag{13}$$

where I_A and I_B are inhibition efficiencies of AMPX and halide respectively; I_{AB} is the inhibition efficiency of a combination of halide and AMPX. Table 4 presents inhibition efficiencies of AMPX when co-employed with 0.006 M KI, KBr and KCl, using gravimetric, gasometric and thermometric methods. Values of S calculated from equation 13 (from gravimetric, gasometric and thermometric data) are presented in Table 5.

Table 5. Synergistic parameters for joint combination of various concentrations of AMPX with 0.06 M KCl, KI and KBr

$C \times 10^{-7}$ (M)	KBr + AMPX	KI + AMPX	KCl + AMPX	KBr + AMPX	KI + AMPX	KCl + AMPX
2	3.74	0.79	43.03	6.71	0.54	3.68
4	1.72	0.84	59.62	6.20	1.10	6.67
6	1.32	0.95	80.37	6.63	0.97	7.08
8	1.00	1.20	71.91	10.39	1.31	6.93
10	0.95	0.84	48.19	23.74	1.80	6.97

The results obtained indicated that at 303 K, the values of S obtained when 0.06 M KBr was added to 0.1, 0.2 and 0.3 g/dm³ of AMPX were greater than one indicating that the increase in inhibition efficiency of AMPX for these concentrations may be due to interaction between molecules of AMPX and KBr. AMPX concentrations of 0.4 and 0.5 g/dm³, the values of S were 1.00 and 0.95 (≈ 1.00) respectively indicating that AMPX and KBr have no effect on each other. When 0.06 M KI was added to different concentrations of AMPX, the values of S were less than unity (except at a concentration of 0.4 g/dm³ where synergism was observed). This indicates that at these concentrations, the adsorption of AMPX or KI on mild steel surface is antagonistic to each other.

At 333 K, synergism was observed for all combinations of AMPX with 0.06 M KBr and 0.06 M KCl indicating that between the concentration range of 0.1 – 0.5 g/dm³, the enhanced inhibition efficiencies may be due to interaction between KBr and AMPX molecules. When different concentrations of AMPX were respectively combined with 0.06 M KI, synergistic effect was obtained at AMPX concentrations of 0.2, 0.4 and 0.5 g/dm³ but at concentrations of 0.1 and 0.3 g/dm³, the values of S were less than unity indicating that the adsorption of AMPX or KI at these concentrations is antagonistic to each other.

At 303 K and 333 K, joint adsorption of AMPX on mild steel surface is found to occur according to Langmuir adsorption isotherm (Figure not shown). This implies that the concentration of

the inhibitor (C_{inh}) is related to its degree of surface coverage according to equations 10 and 11. Therefore, plots of $\log(C/\theta)$ versus $\log C$ yielded straight lines confirming that Langmuir adsorption isotherm is applicable to the joint adsorption of these inhibitors and halides on mild steel surface.

Values of the binding constant (B) calculated from intercepts of the adsorption plots were used to calculate the free energies of adsorption from equation 12. Calculated values of ΔG_{ads} at 303 and 333 K (Table 6) are found to be negatively less than -40 kJ/mol indicating that joint adsorption of AMPX and halides is spontaneous and proceeded via physical adsorption.

Table 6. Thermodynamic parameters for joint adsorption of halides and AMPX

System	ΔG_{ads} (kJ/mol)	ΔH_{ads} (kJ/mol)	ΔS_{ads} (J/mol)	E_a (kJ/mol)
KBr + AMPX	-16.44	-28.34	126.6300	16.3245
KI + AMPX	-14.83	-43.76	170.2160	8.8415
KCl + AMPX	-15.96	-58.19	-163.820	11.2342

In order to calculate the heat of adsorption (Q_{ads}) for the combination of AMPX with halides (KBr, KCl and KI), equation 14 was used [31]:

$$Q_{ads} = 2.303R [\log (\theta_2/1-\theta_2) - \log (\theta_1/1-\theta_1)] \times (T_2T_1)/(T_2 - T_1) \quad 14$$

where θ_2 and θ_1 are degrees of surface coverage at temperatures of 333 K (T_2) and 303 K (T_1) respectively. R is the gas constant. Values of Q_{ads} are expected to be approximately equal to the corresponding enthalpy change because the reactions were carried out at constant pressure [32]. These values are also presented in Table 6. The values are negative for all combinations of inhibitors with 0.06 M KBr indicating that the adsorption of the inhibitor-KBr is exothermic as opposed to positive values earlier obtained for AMPX alone. Negative values were also observed for combinations of KI with AMPX. Values of enthalpy change for the combination of KCl with AMPX were positive indicating that their adsorption is endothermic.

Also, the activation energy for the corrosion of mild steel in the presence of a combination of AMPX and halides (KI, KBr and KCl) was calculated using the modified form of the Arrhenius equation (equation 15);

$$\log(CR_2/CR_1) = E_a/2.303R(1/T_1 - 1/T_2) \quad 15$$

The activation energies calculated from equation 16 are greater than those obtained for inhibition of corrosion by AMPX when they are not combined with halides indicating that there is an increased stability due to halides- AMPX combination. These values (Table 6) are also lower than the threshold value of 80 kJ/mol indicating that joint adsorption of halide and AMPX also favours the

mechanism of charged transferred from the inhibitor's molecule to the charged metal (physical adsorption).

Values of entropy of adsorption (ΔS_{ads}) for combinations of AMPX, with halides (KI, KBr and KCl) were calculated using Gibb Helmholtz equation;

$$\Delta G_{\text{ads}} = \Delta H_{\text{ads}} - T\Delta S_{\text{ads}} \quad 16$$

Calculated values of ΔS_{ads} are also recorded in Table 6. These values are positive for all combinations of 0.06 M KBr and 0.06 M KI with AMPX, but negative for combination of 0.06 M KCl with AMPX. The negative values of ΔS_{ads} indicate that the reaction may be controlled by the activation complex.

3.6 Quantum Chemical study

Table 7 presents calculated values of semi empirical parameters for AMPX using PM6, PM3, AM1, RM1 and MNDO Hamiltonians. The calculated quantum chemical parameters included the energy of the highest occupied molecular orbital (E_{HOMO}), the energy of the lowest unoccupied molecular orbital (E_{LUMO}), the energy gap (ΔE), the total energy of the molecule (TE), the electronic energy of the molecule (EE) and the dipole moments (μ). Several researches have confirmed that these parameters are unique in predicting the reactivity of a molecular species.

Table 7. Calculated quantum chemical parameters for AMPX

Quantum parameters	PM6	PM3	AM1	RM1	MNDO
E_{HOMO} (eV)	-9.06	-8.88	-8.82	-8.75	-8.86
E_{LUMO} (eV)	-1.81	-1.77	-1.48	-1.37	-1.34
ΔE (eV)	7.25	7.11	7.34	7.38	7.52
TE (eV)	-5940.59	-5896.89	-6469.42	-6407.37	-6501.24
EE (eV)	-47598.77	-47255.82	-48123.25	-48199.78	-48169.90
μ (Debye)	7.41	4.93	6.00	6.83	6.35

According to the frontier molecular orbital theory (FMO), the shapes and symmetries of the highest-occupied and lowest-unoccupied molecular orbitals (HOMO and LUMO) are crucial in predicting the reactivity of a species and the stereochemical and regiochemical outcome of a chemical reaction [33]. Therefore, the FMO revealed that the formation of a transition state is due to an interaction between frontier orbitals (HOMO and LUMO) of reacting species [34]. Other quantum chemical parameters such as the total energy of the molecule (TE), the electronic energy of the molecule (EE) and the dipole moments (μ) have also been found to exhibit excellent correlations with experimental inhibition efficiencies [35]. Our present data compares favourable with those obtained by

other researchers for some confirmed corrosion inhibitors. Hence quantum chemical principles can be used to model the corrosion inhibition potentials of AMPX.

Table 8. Fukui function calculated from Mulliken (Lowdin) charges and Huckel charges of atoms in AMPX

	f^+ (e)	f^- (e)	f^0 (e)	Huckel Charge
1 C	-0.0340(-0.0309)	0.0078(0.0070)	-0.0131(-0.0120)	0.0611
2 C	-0.2345(-0.2999)	0.0271(0.0466)	-0.1037(-0.1267)	0.4828
3 N	-0.0339(-0.0367)	0.0051(0.0062)	-0.0144(-0.0153)	0.1068
4 C	-0.0111(-0.0103)	0.0055(0.0063)	-0.0028(-0.0020)	0.1112
5 C	-0.0039(-0.0080)	-0.0021(-0.0019)	-0.0030(-0.0050)	0.0621
6 C	0.0079(0.0050)	-0.0004(-0.0009)	0.0038(0.0021)	0.0759
7 S	-0.1087(-0.0989)	0.0091(0.0088)	-0.0498(-0.0451)	0.0036
8 C	-0.0054(-0.0088)	-0.0020(-0.0020)	-0.0037(-0.0054)	-0.0945
9 C	-0.0012(-0.0023)	-0.0011(-0.0010)	-0.0012(-0.0016)	-0.1061
10 C	-0.0555(-0.0670)	0.0121(0.0129)	-0.0217(-0.0271)	0.6527
11 O	0.0393(0.0541)	-0.0172(-0.0177)	0.0110(0.0182)	-0.7127
12 O	0.0081(0.0048)	0.0035(0.0032)	0.0058(0.0040)	-0.1597
13 O	-0.1494(-0.1455)	-0.0881(-0.1032)	-0.1188(-0.1243)	-0.7745
14 N	-0.0095(-0.0115)	0.0044(0.0061)	-0.0026(-0.0027)	0.1728
15 C	-0.0798(-0.1049)	0.0673(0.0951)	-0.0062(-0.0049)	0.4696
16 C	0.0246(0.0368)	-0.0402(-0.0530)	-0.0078(-0.0081)	-0.0208
17 O	0.0985(0.1197)	-0.1420(-0.1615)	-0.0217(-0.0209)	-0.8439
18 C	-0.0227(-0.0345)	0.0026(0.0169)	-0.0100(-0.0088)	0.0403
19 C	0.0021(0.0035)	-0.0278(-0.0313)	-0.0129(-0.0139)	-0.0452
20 C	-0.0145(-0.0210)	-0.0126(-0.0064)	-0.0136(-0.0137)	-0.0309
21 C	0.0126(0.0176)	-0.1025(-0.1210)	-0.0450(-0.0517)	0.0151
22 C	-0.0171(-0.0233)	-0.0259(-0.0217)	-0.0215(-0.0225)	-0.0380
23 C	0.0015(0.0033)	-0.0017(-0.0023)	-0.0001(0.0005)	0.0659
24 N	-0.0085(-0.0087)	-0.0011(-0.0018)	-0.0048(-0.0053)	-0.2916
25 C	-0.0146(-0.0188)	-0.1297(-0.1631)	-0.0722(-0.0909)	0.1954
26 O	-0.0176(-0.0237)	-0.0525(-0.0423)	-0.0351(-0.0330)	0.0740
27 N	0.0065(0.0150)	-0.0878(-0.0962)	-0.0406(-0.0406)	-0.2118
28 C	0.0079(0.0043)	-0.0194(-0.0175)	-0.0057(-0.0066)	0.1074
29 C	0.0251(0.0313)	-0.1382(-0.1571)	-0.0566(-0.0629)	-0.2033
30 C	0.0115(0.0130)	-0.0207(-0.0174)	-0.0046(-0.0022)	-0.0712
31 C	0.0048(0.0028)	-0.0017(0.0009)	0.0015(0.0018)	0.1637
32 C	0.0032(0.0032)	-0.0147(-0.0160)	-0.0057(-0.0064)	-0.0722
33 C	-0.0034(-0.0068)	-0.0073(-0.0045)	-0.0054(-0.0056)	-0.0284
34 C	-0.0016(-0.0044)	-0.0105(-0.0075)	-0.0061(-0.0060)	-0.0734
35 C	0.0049(0.0051)	-0.0121(-0.0110)	-0.0036(-0.0029)	-0.0323
36Cl	-0.0094(-0.0082)	-0.0231(-0.0215)	-0.0163(-0.0148)	0.0279

The Fukui function is an index that has widely been used in corrosion studies for distinguishing each part of a molecule on the bases of its chemical behaviour. According to Stayanov et al. [36], the Fukui function is motivated by the fact that if a fraction of electron, δ is transferred to an N electron molecule, it will tend to distribute so as to minimize the energy of the resulting N + δ electron system. The resulting change in electron density is the nucleophilic and electrophilic Fukui functions, which can be defined base on the Finite difference approximation as follows [37];

$$f^+ = q(N) - q(N-1) \quad 17$$

$$f^- = q(N+1) - q(N) \quad 18$$

where $q(N)$ is the Mulliken (Lowdin)'s charge on the atom with N electron and $q(N-1)$ and $q(N+1)$ are the charges on the atom of the molecule with N-1 and N+1 electrons respectively. Equations 17 and 19 are the major expressions for condensed Fukui function, which is the most applicable form of the Fukui model. From the application of the frontier orbital theory of reactivity of Fukui, three different functions can be obtained. The function, f^+ is associated with the LUMO and measures reactivity towards a donor reagent, the function f^- is associated with the HOMO and measures reactivity toward an acceptor reagent and finally, the average of both, f^0 , measures reactivity toward a radical. In Table 8, calculated values of f^+ , f^- and f^0 are presented. Also presented, are calculated values of Huckel charges on atoms of AMPX. The presented data is devoid of those obtained for hydrogen atoms. From the results obtained, it can be stated that the site for nucleophilic attack is where the value of f^+ is maximum. On the other hand, the site for electrophilic attack is controlled by the value of f^- . Therefore, in AMPX, the possible active sites for electrophilic attacks are N3, S7, O11, O12, O13, N14, O17, N24, O26 and N27.

Table 9. Energy of protonation, proton affinity and interaction energies for AMPX

Hetero atoms	E_{Pro} (eV)	PA (eV)	$E_{(\text{Fe-X})}$ (eV)	E_{int} (eV)
N3	3.172352	-0.6684		
S7	3.448641	-0.3921	4.6945	29.0450
O11	3.398017	-0.4427	3.3535	-1.8782
O12	3.482459	-0.3583	3.3967	-0.8822
O13	3.530972	-0.3098	2.9912	-10.2345
N14	3.483936	-0.3568	3.4344	-0.0124
O17	3.374332	-0.4664	3.3011	-3.0863
N24	3.483789	-0.3570	3.4066	-0.6539
O26	3.356073	-0.4847	0.0000	-79.2121
N27	6.421921	2.5812	3.0808	-8.1673

For nucleophilic attack, the active site is expected to be one of the carbon atoms (C16) but radical attack is expected to take place at any of the listed sites. From the results obtained from Fukui function and Huckel charges analysis, it is indicative that the site for electrophilic attack is in the amide nitrogen (i.e N14).

Similarly, the site for nucleophilic attack is the aromatic ring carbon atom (C16) while the prefer site for radical attack is in the carbonyl oxygen (O11). It should be pointed out that the inhibition effect of a corrosion inhibitor is usually attributed to the adsorption of the inhibitor on the metal surface via the active centre. Adsorption caused by Van der Waals and Coulombic interactions are described as physical adsorption, whereas that resulted from interaction between the π -electron of organic molecules and d-orbital of metal correspond to chemical adsorption. Inevitably, physical adsorption proceeds chemical adsorption. After physical adsorption, the inhibitor's molecules are adsorbed onto the metal surface. Therefore, estimation of the binding energy of the inhibitor to the metal, hence the interaction energy can furnish information on the possibility of adsorption.

According to Sahin et al. [38], the interaction energy between and inhibitor and the metal surface can be calculated using the following equation;

$$E_{\text{int}} = E_{(\text{Fe-X})} - (E_x + E_{\text{Fe}}) \quad 19$$

where E_{Fe} is the total energy of the iron atom and E_x is the total energy of the inhibitor. When the adsorption occurs between the inhibitor and Fe, the energy of the new system is expressed as $E_{(\text{Fe-X})}$. Table 9 presents values of calculated E_{int} for all possible adsorption sites. From the results obtained, it is evident that values of E_{int} are negative for all the sites implying that the adsorption of AMPX on mild steel surface is spontaneous. Also, from thermodynamic point of view, every system prefers the lowest energy state. Therefore, the lower the values of E_{int} , the more stable the formed complex is expected to be. This assertion also favours the amide nitrogen (N14) as the site for adsorption.

In acidic medium, AMPX can be protonated. All possibilities for protonation at the active sites were considered. The proton affinity (PA) of the inhibitor was calculated for all active sites using the following equation [39];

$$\text{PA} = E_{\text{prot}} - (E_{\text{non-prot}} + E_{\text{H}^+}) \quad 20$$

where $E_{\text{non-prot}}$ and E_{prot} are the energies of the non protonated and protonated inhibitor respectively. E_{H^+} is the energy of H^+ which was calculated as

$$E_{\text{H}^+} = E_{(\text{H}_3\text{O})^+} - E_{(\text{H}_2\text{O})} \quad 21$$

Results obtained from the calculations are also presented in Table 9. From the results obtained, it is evident that the protonation is a downhill exothermic reaction indicating that AMPX has a tendency to be protonated at the amide nitrogen (N14) and at the carbonyl oxygen (O13). This is because the total energy of the protonated system that gives the lowest energy upon protonation is in the O13 and N14. We also observed that the bond lengths between N14-C15, N14-H47 and C1-N14

after protonation were shorted by 0.1577, 0.0845 and 0.1474 Å respectively. This also indicates that there is conjugation during protonation.

In Fig.7, the HOMO and LUMO molecular orbital diagrams of AMPX and Fe-AMPX adsorbed complex are presented. The plot confirms the findings that AMPX is adsorbed on mild steel surface via N14.

Optimised structure

HOMO

LUMO

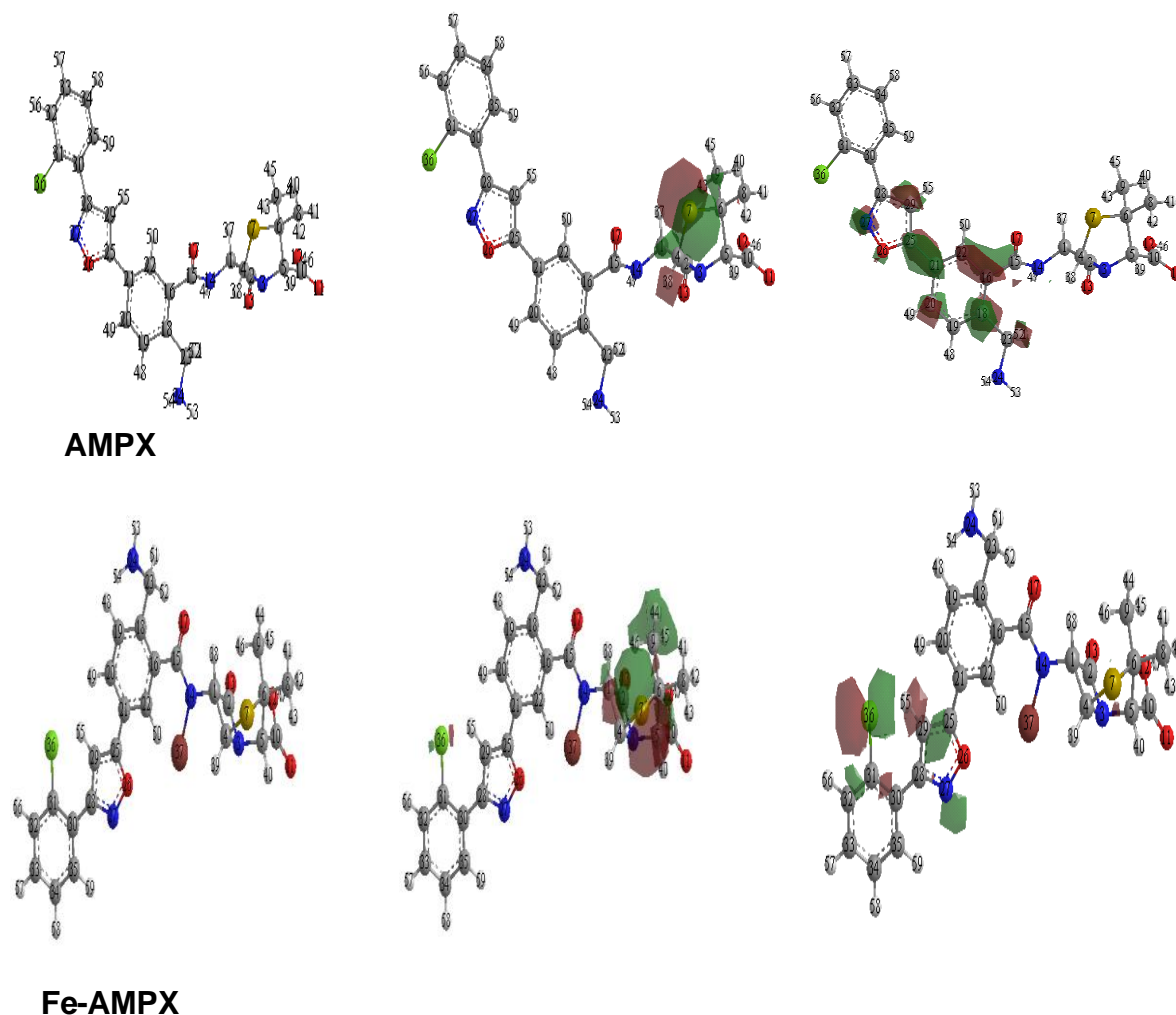


Figure 7. Optimised structure, HOMO and LUMO molecular orbital of AMPX and Fe- AMPX

4. CONCLUSIONS

From the results and findings of the study, AMPX is a good adsorption inhibitor for the corrosion of mild steel. The inhibitor is spontaneously adsorbed on mild steel surface via the amide nitrogen (N14). The inhibitor is protonated in acidic medium before adsorption. Quantum chemical

principles can be used to study the inhibitory behaviour of this inhibitor. The use of AMPX as an inhibitor for the corrosion of mild steel in acidic medium is advocated in this work.

ACKNOWLEDGEMENTS

The authors are grateful to Dr. R. S. Stayanov of the Canadian Institute of Nanotechnology and to Mr. Patrick Ukat for their technical supports. EEE acknowledges the support of the National Research Foundation (NRF) of South Africa for funding.

References

1. M.A. Amin, Q. Mohsen, O.A. Hazzazi, *Mater. Chem. Phys.* (2009) 908.
2. R. Laamari, J. Benzakour, F. Berrekhis, A. Abouelfida, A. Derja, and D. Villemin, *Arabian Jour. of Chem.* 4(2011) 271.
3. S.S. Abdel-Rehim, K.F. Khaled, and N.A. Al-Mobarak, *Arabian Jour. of Chem.* 4(2011) 333.
4. S.A. Umoren, I.B. Obot, E.E. Ebenso and N.O. Obi-Egbedi, *Desalination* 250 (2009) 225.
5. J.D. Talati, M.N. Desai and N.K. Shah, *Mater. Chem. Phys* 93 (2005) 54.
6. N.O. Eddy, E.E. Ebenso and U.J. Ibok, *J. Applied. Electrochem* 40(2010) 445.
7. N.O. Eddy, U.J. Ibok and B.I. Ita, *Jour. Computational Methods Sci. & Eng.*, 9(2010) 1.
8. N.O. Eddy and E.E. Ebenso, *Int. Jour. Electrochemical Sci.* 5 (2010) 731.
9. N.O. Eddy and S.A. Odoemelam, *Pigment and Resin Technology* 38(2009) 111.
10. N.O. Eddy, S.A. Odoemelam and A.O. Odiongenyi, *Green Chem. Letters & Reviews* 2 (2009) 111.
11. N.O. Eddy, U.J. Ibok, E.E. Ebenso, *Anales des la Asociacion Quimica Argentina* 97 (2009) 178.
12. N.O. Eddy, U.J. Ibok, E.E. Ebenso, Ahmed El Nemr, and El Sayed H.El Ashry. *J. Molecular Modeling.* 15(2009) 1085.
13. N.O. Eddy, P.A. Ekwumengbo, P.A.P. Mamza, *Green Chem. Letters and Reviews* 2(2009) 223.
14. N.O. Eddy and P.A.P. Mamza, *Portugaliae Electrochimica. Acta.* 27(2009) 20.
15. A. Yurt, A. Balabam, S.U. Kandemer, G. Bereket and B. Erk, *Mater. Chem. Phys* 85 (2004) 420.
16. N.O. Eddy, S.A. Odoemelam and A.O. Odiongenyi, *Green Chem. Letters & Review* 2 (2009) 111..
17. H. Ashassi-sorkhabi, B. Shaabani, B. Aligholipour and D. Seifzadeh, *Applied Surface Science* 252 (2006) 4039.
18. M. Abdallah, *Corros. Sci.* 46 (2004) 1981.
19. H.M.A. Soliman and H.H. Abdel-Rahman, *Jour. Braz. Chem. Soc.* 17(2006) 705.
20. N.O. Eddy, S.A. Odoemelam and A.O. Odiongenyi, *Jour. Applied. Electrochem.* 39(2009) 849.
21. M. Abdallah, *Corros. Sci.* 44(2002) 717.
22. L. Bilgic and N. Caliskan, *J. Applied Electrochem.* 31 (2001) 79.
23. E.E. Ebenso, *Mater. Chem. Phys* 79 (2003) 58.
24. N.O. Eddy and A.O. Odiongenyi, *Pigment and Resin Technology* 38 (2010) 288.
25. T. Arslan, F. Kandemirli, E. E. Ebenso, I. Love, H. Alemu, *Corros. Sci.* 51(2009) 35.
26. Y. Yan, W. Li, L. Cai and B. Hou, *Electrochimica Acta* 53(2008) 5953.
27. K.C. Emergull, E. Duzgun and O. Atakol, *Corros. Sci.* 48(2005) 3243.
28. N.O. Eddy, S.R. Stoyanov, E.E. Ebenso, *Int. Jour. Electrochemical Sci.* 5(2010) 1127.
29. S.A. Umoren, O. Ogbobe and E.E. Ebenso, *Trans. of the SAEST*, 41(2006) 74.
30. M. Ehteschamzade, T. Shahrabi, M.G. Hosseni, *Appl. Surf. Sci.* 252(2005) 2949.
31. N.O. Eddy and B.I. Ita, *Journal of Molecular Modeling* 17(2010) 359..
32. N.O. Eddy, *Pigment and Resin Technology* 39 (2010) 348.
33. N.O. Eddy, *Journal of Advanced Research* 2(2010) 35.
34. H. Wang, X. Wang, H. Wang, L. Wang and A. Liu, *Jour. Molecular Modelling* 13(2007) 147.
35. G. Gao and C. Liang, *Electrochimica Acta* 52(2007) 4554.

36. R.S. Stayanov, S. Gusarov and A. Kovalenko, *Molecular Simulation* 34(2008) 943.
37. P. Fuentealba, P. Perez, R. Contreras, *Jour. Chemical Physics* 113(2000) 2544.
38. G. Sahin, F. Karci and S. Bilgic, *Journal of Applied Electrochemistry* 38(2008) 809.
39. M.S. Masound, M.K. Awad, M.A. Shaker and M.M.T. El-Tahawy, *Corros. Sci.* 52(2010) 2387.